Finite Elements in Analysis and Design 220 (2023) 103936

Contents lists available at ScienceDirect

Finite Elements in Analysis & Design

journal homepage: www.elsevier.com/locate/finel

A new locking-free finite element for N-layer composite beams with interlayer slips and finger joints

Barbara Fortuna [a,*], Goran Turk [a], Simon Schnabl [a,b]

[a] University of Ljubljana, Faculty of Civil and Geodetic Engineering, Jamova 2, Ljubljana, 1000, Slovenia
[b] University of Ljubljana, Faculty of Chemistry and Chemical Technology, Večna pot 113, Ljubljana, 1000, Slovenia

ARTICLE INFO

Keywords:
Beam theory
Partial interaction
Finger joint
Beech wood
Slip and shear locking
Experimental testing

ABSTRACT

This paper presents the formulation of strain-based finite elements for modelling composite beams with finger joints considering slip between the layers. The finite elements are derived according to Reissner beam theory based on the modified principle of virtual work where the displacements and rotations are eliminated from the problem and the axial deformation, shear deformation and curvature of the layers remain only functions to be approximated within the finite element. Lagrange polynomials are used as shape functions to approximate the deformations and various interpolation methods are applied to numerical examples, with the Lobatto integration scheme giving slightly better results than Equidistant. The experimentally measured mechanical properties needed as input data for the numerical model are given for the four glued laminated beech beams. The numerical model is thoroughly verified and validated. The results show that the presented finite element formulation is an efficient tool for practical and accurate calculations.

1. Introduction

Composite structures in general offer a wide range of possibilities, and the application to structural elements made of wood is only one of them. Such use of wood results in strong, stable and reliable structural elements. Glued laminated beams, along with laminated veneer lumber and cross-laminated timber, are one of the most commonly used forms of wood composites, where different types of adhesives are used as a second material. With the adhesive layer between the wood layers, a continuous interlayer contact is made between the layers to achieve a strong and rigid bond between the wood layers. However, in reality, adhesives are deformable and neglecting the deformation of the interlayer contact can lead to an incorrect estimation of the mechanical response of the composite beams under load, which is why the implementation of interlayer slip is important. Newmark's theory [1] is one of the best known theories for composite beams with partial interaction between layers. As applicable as the composite structural elements are, the subject has been further investigated by many researchers for different levels of complexity of the models. Goodman and Popov [2] showed the numerical model for a layered beam with deformable connection between layers considering linear materials. In general, wood can be described as a linear-elastic material [3,4] when loaded in tension, for example, but other materials such as steel and concrete or their composites show pronounced non-linear behaviour. Moreover, large deformations of the structural elements require more precise non-linear analysis, so other models for non-linear materials with geometric nonlinearity [5–10] have been developed. Some of the models are based on Bernoulli beam theory and neglect the shear deformation of the layers [9,11,12], while others take into account more accurate stress and displacement fields and thus shear deformation [13–19]. In general, shear stresses are not constant across the thickness of layers and higher order beam theories have been developed to account for the distribution of shear stresses in plates and beams [20–22]. One of useful approaches to solve higher order beam problems is the Carrera Unified Formulation (CUF) which was first developed for solid plates and shells [23–25] and has been revised and adapted in the last decade to solve complex geometric non-linear problems of laminated composites including beams [26–28]. The method can be used to describe challenging three-dimensional problems with one-dimensional and two-dimensional finite elements. It is reported to give accurate results for complex problems with relatively low computational time and can also be used for dynamic problems. Due to the typical geometry of the beam, where one dimension is much larger than the other two, most models have been derived as planar models, but there are also some studies that analyse the beam with interlayer slip as a three-dimensional problem [15,29–31]. For composite beams with a small number of layers and linear material properties, explicit analytical solutions can be found [11,32–34], while numerical methods are used for

* Corresponding author.
E-mail address: bfortuna@fgg.uni-lj.si (B. Fortuna).

https://doi.org/10.1016/j.finel.2023.103936
Received 16 September 2022; Received in revised form 24 February 2023; Accepted 2 March 2023
Available online 16 March 2023

non-linear materials. [5–10,12,35–38]. For glued laminated beams, the boards in layers must be connected with structural finger joints [39]. Finger joints often represent a weak point in the structural element and therefore play an important role in the mechanical response of the glued laminated beam and according to the literature overview, there is no model that would be developed according to the beam theory that would consider the presence of finger joints in the composite beam.

One of the best known models for glued laminated beams with finger joints is the Karlsruhe model [40–42], which is an improved version of a model presented by Foschi and Barrett [43]. The Karlsruhe model takes into account the non-linear behaviour only in compression while failure can occur only in layers loaded in tension. The positions and mechanical properties of the finger joints are generated stochastically. However, the model does not consider the interlayer slip and shear deformations of the beam.

Displacement-based finite element formulations are often used in numerical methods [35,36,44–47], but their main drawback is that the problem of inconsistency of the displacement field may occur, leading to slip-locking of the model [48]. Strain-based finite elements [36] have proven to provide an efficient solution to this problem [49]. Shear locking is also one of the phenomena that occur when thin and slender structural elements are modelled with displacement-based finite elements formulated for the analysis of thick and stiff structural elements [22,50]. This problem is solved with various approaches that usually alternate the integration scheme [22,51,52]. Another solution to eliminate the problem of shear locking is called Mixed Interpolation of Tensorial Components (MITC) and presented in [53,54]. It essentially uses the combination of interpolating displacements and shear strains of shells and plates. This approach has recently been extended to higher order beam theories [55] and has been shown to be efficient. When the finite element formulation is based entirely on interpolating strains instead of displacements, the problems of shear-locking are also eliminated [49]. However, in the literature no displacement- or strain-based finite element formulation for composite beams, that would consider slip between the layers and finger joints in the layers of the beams, can be found.

Thus, the objective of this paper is to present a novel type of strain-based finite element specifically designed for the numerical modelling of composite beams with finger joints, which takes into account the interlayer slip and the shear deformations of the layers without being constrained by the number of layers or the number of finger joints. The model is primarily designed for modelling glulam beams with layers with similar shear properties. The materials used in the model can be linear or non-linear materials. The calculations are fast and efficient and provide accurate results.

2. Formulation of basic equations of a N-layer composite beams

The formulation of the equations is based on the kinematically exact Reissner theory for planar beams [56]. The deformation of the beam is limited to small displacements and small rotations and shear deformation of the layers is taken into account so the originally straight cross-sections in the undeformed state remain straight but not perpendicular to the reference axis in the deformed configuration. The basic subject of our problem is a geometrically linear composite beam with an arbitrary number of layers N, see Fig. 1, subjected to the generalized load $\mathcal{P}$ as shown in Fig. 1. The layers are denoted by i, where $i = \{1, 2, \dots, N\}$. They are connected with interlayer contact layer, which has negligible thickness and known material properties. The interlayer contact is continuous along the length of the beam L_{beam}. All layers are initially undeformed and have the same length, i.e. $L^i = L_{beam}$. The beam is defined in Cartesian space $\mathbb{R}^3 = \{X, Y, Z\}$ with fixed orthonormal global basis vectors $\mathbf{E}_X, \mathbf{E}_Y$ and $\mathbf{E}_Z$, where $\mathbf{E}_Z = \mathbf{E}_X \times \mathbf{E}_Y$. The global reference axis of the straight, undeformed beam is assumed to be at the lowest edge of the beam. For simplicity, the reference axis coincides with the X axis of the global coordinate system and the reference axes of all layers are identical to the global reference axis. The arbitrary particle of layer i is defined with material coordinates (x^i, y^i, z^i). The shape of the cross-section A^i of layer i is considered prismatic, defined with thickness h^i and width b in the plane Y, Z. The cross-sections of the layers are homogeneous and their shape does not change during deformation. In general, the displacement of any particle of the beam with coordinates (x^i, y^i, z^i) is described by the position vector $\mathbf{R}^{\mathbf{i}}(x^i, y^i, z^i)$ as shown in Fig. 2 and written as follows:

$$\mathbf{R}^i(x^i, z^i) = \left(x^i + u^i(x^i) + z^i\,\varphi^i(x^i)\right)\mathbf{E}_X + \left(z^i + w^i(x^i)\right)\mathbf{E}_Z. \tag{1}$$

where $u^i(x^i)$ and $w^i(x^i)$ are the horizontal and vertical displacements of the particle at the reference axis of layer i in the X and Z directions, respectively, the $\varphi^i(x^i)$ represents the rotation in the XZ plane and defines the position of the arbitrary particle of the cross-section.

In this way, the deformed configuration of the beam is kinematically described by the basic kinematic functions $u^i(x^i)$, $w^i(x^i)$, and $\varphi^i(x^i)$. The deformations of the layers are generally dependent and constrained to each other. A partial interaction is defined between the layers, where the connection between the layers is deformable and has known stiffness properties. In this work, the partial interaction of the layers is limited to sliding between the layers, while delamination is restricted in the transverse direction, see Fig. 2. This is defined with the equation:

$$\mathbf{R}^i(x^i, y^i, z^j) = \mathbf{R}^{i+1}(x^{i+1}, y^{i+1}, z^j), \tag{2}$$

where $i = \{1, 2, \dots, N\}$ and $j = \{1, 2, \dots, N-1\}$. $\mathbf{R}^i$ and $\mathbf{R}^{i+1}$ are the position vectors of arbitrary particles T^i and T^{i+1} in layers i and $i+1$, respectively. They are chosen to have different positions in the undeformed configuration, but the same position after deformation, see Fig. 2.

Considering $y^i = y^{i+1} = 0$ in Eq. (1) and the fact that two adjacent layers i and $i+1$ share the same contact j, $z^i = z^{i+1} = z^j$, the Eq. (2) is written:

$$\begin{aligned}&\left(x^i + u^i(x^i) + z^j\,\varphi^i(x^i)\right)\mathbf{E}_X + \left(z^j + w^i(x^i)\right)\mathbf{E}_Z\\ =&\left(x^{i+1} + u^{i+1}(x^{i+1}) + z^j\,\varphi^{i+1}(x^{i+1})\right)\mathbf{E}_X + \left(z^j + w^{i+1}(x^{i+1})\right)\mathbf{E}_Z,\end{aligned} \tag{3}$$

or in rearranged component form as

$$x^i - x^{i+1} + u^i(x^i) - u^{i+1}(x^{i+1}) + z^j\left(\varphi^i(x^i) - \varphi^{i+1}(x^{i+1})\right) = 0, \tag{4}$$

$$w^i(x^i) - w^{i+1}(x^{i+1}) = 0. \tag{5}$$

Eq. (5) defines that no delamination between the layers is allowed. The deformation of the interlayer contact between particles T^i and T^{i+1} with coordinates x^i and x^{i+1}, respectively, on the undeformed reference axes is now defined only by the interlayer slip $\Delta^j_X(x^i)$:

$$\Delta^j_X(x^i) = x^i - x^{i+1} \neq 0, \tag{6}$$

$$\Delta^j_Z(x^i) = 0. \tag{7}$$

If the expression for the slip $\Delta^j_X(x^i)$ in the interlayer contact j is implemented into Eq. (4), the following equation is obtained:

$$\Delta^j_X(x^i) = u^{i+1}(x^{i+1}) - u^i(x^i) + z^j\left(\varphi^{i+1}(x^{i+1}) - \varphi^i(x^i)\right). \tag{8}$$

In civil engineering, the expected deformation of structural elements is limited by the serviceability limit state, therefore displacements and rotations are small. Furthermore, similar assumptions can be considered for the interlayer slips. The connection between layers in structural elements usually has a relatively high stiffness, so that the expected interlayer slips are also small. Such simplifications are often used [12, 14,34,57]. Based on Eq. (5) and the assumption of small displacements, rotations and deformations, it follows that the vertical displacements of layers of a given cross-section can be considered equal:

$$w^i(x^i) = w^{i+1}(x^{i+1}) = w(x). \tag{9}$$

Taking into account Eq. (9), we further assume that also the rotations φ^i and pseudocurvatures κ^i are the same for all layers i, where $i =$

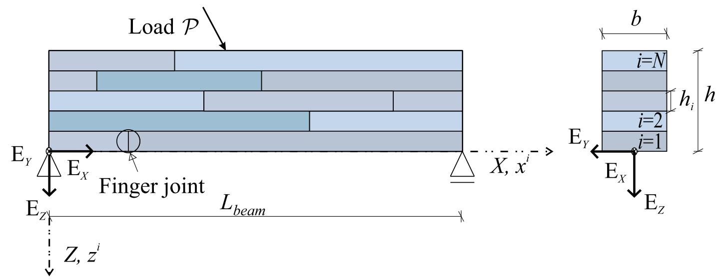

Fig. 1. Model of a composite beam with arbitrary number of layers N and arbitrary number of finger joints in the layers.

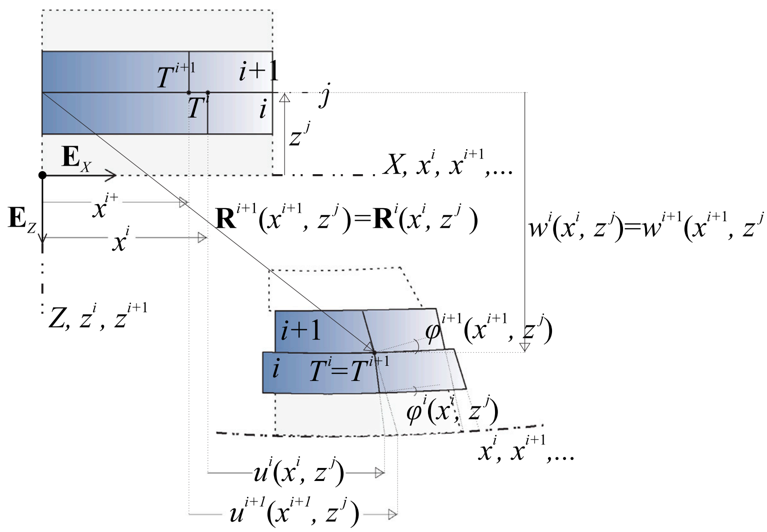

Fig. 2. A schematic presentation of the geometry of the slips between the layers i and $i+1$ in interlayer contact j.

$\{1, 2, \ldots, N\}$ and N is the total number of layers. The layers deform uniformly in the transverse direction and the shear deformations γ^i are also identical for all layers:

$$\varphi^i(x^i) = \varphi^{i+1}(x^{i+1}) = \varphi(x), \tag{10}$$

$$\gamma^i(x^i) = \gamma^{i+1}(x^{i+1}) = \gamma(x), \tag{11}$$

$$\kappa^i(x^i) = \kappa^{i+1}(x^{i+1}) = \kappa(x). \tag{12}$$

In this way, the number of unknowns is reduced and these assumptions simplify the model considerably. It should be emphasized, however, that these assumptions are fully justified only for the cases where the shear moduli of the layers G^i are equal. In all other cases there is a discrepancy in the results compared to those obtained without the assumption of equal shear deformations, but in the case of glulam beams this is within 5% and therefore negligible.

Kinematic equations:

Based on the Reissner planar beam theory [56], the kinematic equations are defined to relate the kinematic quantities, i.e., the displacements and the rotations are related to the deformations ε^i, γ^i and κ^i of the layer i and vice versa. According to the Reissner beam theory [56], the kinematic equations in general form are a first-order differential equations and can be used to solve mechanical problems regardless to the magnitude of displacements and rotations and have been presented in detail in the past [5,14,58]. However, due to the assumption of small displacements and rotations, the geometry of the structural element does not change significantly during deformation. With the consistent linearization [59,60] and considering Eqs. (10)–(12), the generalized kinematic equations can be simplified and written as linear first-order differential equations:

$$\frac{du^i(x)}{dx} - \varepsilon^i(x) = 0, \tag{13}$$

$$\frac{dw(x)}{dx} + \varphi(x) - \gamma(x) = 0, \tag{14}$$

$$\frac{d\varphi(x)}{dx} - \kappa(x) = 0. \tag{15}$$

The deformations in Eq. (13)–(15) are the longitudinal deformation of the material, $\varepsilon^i(x)$, the shear deformation, $\gamma(x)$, and the pseudocurvature or bending deformation, $\kappa(x)$, of the cross-section of the beam. When $\gamma(x) = 0$, the $\varepsilon^i(x)$ also represents the specific change in length of the reference axis of the layer i, and when $\varepsilon^i(x) = 0$, the pseudocurvature κ represents the actual curvature of the reference axis of the layers [6,61]. The longitudinal deformation D^i of the material at an arbitrary position over the height of the beam can be determined with the following equation:

$$D^i(x, z^i) = \varepsilon^i(x) + z^i\,\kappa, \tag{16}$$

where $i = \{1, 2, \ldots, N\}$.

Equilibrium equations:

The equilibrium equations are used to connect the internal forces and moments caused by the external load. For multilayer elements there are two types of loads acting on each layer i. The external distributed load $\mathbf{p}^i_{ex}(x) = p^i_{ex,X}(x)\,\mathbf{E}_X + p^i_{ex,Z}(x)\,\mathbf{E}_Z$ and $\mathbf{m}^i_{ex}(x) = m^i_{ex,Y}(x)\,\mathbf{E}_Y$, and the load induced by adjacent layers and transmitted through the contact between layers and therefore called *contact* load, $\mathbf{p}_c^i(x) = p_{c,X}^i(x)\,\mathbf{E}_X + p_{c,Z}^i(x)\,\mathbf{E}_Z$ and $\mathbf{m}_c^i(x) = m_{c,Y}^i(x)\,\mathbf{E}_Y$, where the subscripts "$ex$" and "$c$" denote the applied external and contact contributions, respectively. Furthermore, the external load can either be distributed along an arbitrarily long section of the beam $L_P \in [0, L_{beam}]$ or concentrated to one point as concentrated force P, which can be applied only at the end of the beam element.

As already indicated, the multilayer beams consist of N layers whose mechanical behaviour is interdependent. Therefore, deformation of one layer causes deformation of the other layers. Laminated beams with N layers have $N-1$ interlayer contact surfaces. The notation $j = \{1, 2, \ldots, N-1\}$ is used to denote the contact area between layers and it is assumed that for $i < N$, $i = j$, so that the contact area at the top of the layer has the same notation as the layer. This means that for the first layer $i = 1$, the contact tractions $p_{c,X}^{i,j-1}(x)$ and $p_{c,Z}^{i,j-1}(x)$ are equal to 0. In this way, the traction in the contact surface j acts on the layers i and $i+1$, as shown in Fig. 3. Similarly as kinematic equations (13)–(15), the equilibrium equations in Y and Z directions written about the reference axis of the composite beam can be simplified:

$$\frac{dN^i(x)}{dx} + p_{ex,X}^i(x) + p_{c,X}^{i,j}(x) - p_{c,X}^{i,j-1}(x) = 0, \tag{17}$$

$$\frac{dQ(x)}{dx} + \sum_{i=1}^{N} p_{ex,Z}^i(x) = 0, \tag{18}$$

$$\frac{dM(x)}{dx} - Q(x) + \sum_{i=1}^{N} m_{ex,Y}^i(x) = 0, \tag{19}$$

where $Q(x)$ and $M(x)$ are the total shear force and the total bending moment, respectively:

$$Q(x) = \sum_{i=1}^{N} Q^i(x), \tag{20}$$

$$M(x) = \sum_{i=1}^{N} M^i(x). \tag{21}$$

Note that all equilibrium forces $N^i(x)$, $Q^i(x)$, $M^i(x)$, $Q(x)$, and $M(x)$ in Eqs. (17)–(21) are expressed about the reference axis of the beam (see Fig. 3). The kinematic aspect of the mechanical behaviour of the interlayer contact is described by Eq. (8). Like the material of the layers, the material of the interlayer contact can deform arbitrarily, e.g., elastic, plastic, hyperelastic, etc. The behaviour is defined by the constitutive law of the interlayer contact. This information, similar to the constitutive laws of the layers, is also determined by experimental tests. In general, the results of the tests are arbitrary constitutive functions S_X^j and S_Z^j, where $j = \{1, 2, \ldots, N-1\}$. Since delamination, i.e., the separation of the layers in the transverse direction is neglected in this model, Eq. (5), only the constitutive law for the horizontal component of slip is defined:

$$p_{c,X}^{i,j}(x) = S_X^j\, \Delta_X^j(x). \tag{22}$$

The simplest form of the constitutive lay applies to the linear-elastic interlayer contact and is associated with a constant stiffness value K_X^j. Then the contact traction is defined as:

$$p_{c,X}^{i,j}(x) = K_X^j\, \Delta_X^j(x). \tag{23}$$

Constitutive equations

For the beam to be in static equilibrium, the internal forces and moments induced by the external load must be undertaken by the material of the composite beam. The constitutive equations describe the relationship between the deformation of the beam and the internal forces. Therefore, the general form of the constitutive equations for layer $i = \{1, 2, \ldots, N\}$ is presented by Eqs. (24)–(26), taking into account the assumption of a homogeneous cross-section of the layers.

$$N^i(x) = N_C^i\Big(\varepsilon^i(x), \kappa^i(x)\Big) = \int_{\mathcal{A}^i} \sigma^i(x, z^i)\, dA = \int_{\mathcal{A}^i} \sigma^i\Big(D^i(x, z^i)\Big)\, dA, \tag{24}$$

$$Q^i(x) = Q_C^i\Big(\gamma^i(x)\Big) = \int_{\mathcal{A}^i} \tau^i(x, z^i)\, dA = \int_{\mathcal{A}^i} \tau^i\Big(\gamma^i(x, z^i)\Big)\, dA, \tag{25}$$

$$M^i(x) = M_C^i\Big(\varepsilon^i(x), \kappa^i(x)\Big) = \int_{\mathcal{A}^i} z^i\, \sigma^i(x, z^i)\, dA = \int_{\mathcal{A}^i} z^i\, \sigma^i\Big(D^i(x, z^i)\Big)\, dA. \tag{26}$$

The N_C^i, Q_C^i and M_C^i are the constitutive axial and shear forces and the constitutive bending moment of layer i, respectively, and are defined as the resultants of the normal and shear components of the stress tensor. The stress tensor consists of the normal stress σ^i and the shear stress τ^i and can be expressed by constitutive functions of the material $\mathcal{F}_1^i$ and $\mathcal{F}_2^i$:

$$\sigma^i(x, z^i) = \mathcal{F}_1^i\Big(D^i(x, z^i)\Big), \tag{27}$$

$$\tau^i(x, z^i) = \mathcal{F}_2^i\Big(\gamma(x, z^i)\Big), \tag{28}$$

which are determined by uniaxial compression and/or tensile tests and experimental shear tests and generally describe any material model (linear elastic, hyperelastic, plastic, etc.).

The kinematic equations (13)–(15), the equilibrium equations (17)–(19), and the constitutive equations (24)–(26), represent the fundamental system of $6\,N$ first-order linear differential equations and $3\,N$ algebraic equations requiring $6\,N$ unknown integration constants. To obtain the complete solution for the unknowns u^i, w^i, φ^i, N^i, Q^i, and M^i, the boundary conditions must be defined. As the name implies, the boundary conditions define selected mechanical quantities at the boundaries of the layers, i.e., $x = 0$ and $x = L$, where L represents the length of the finite element. They are usually predefined by the geometry of the model (e.g., the type of supports), but using only one type of boundary conditions does not necessarily lead to a unique solution of the system. Therefore, a combination of Neuman (natural) and Dirichlet (essential) boundary conditions must be used. For each degree of freedom, only one of the two types of the boundary conditions may be used, either Neuman's or Dirchlet's. This is determined by Eqs. (29)–(34) at the boundaries of the layers of the finite element.

Boundary conditions:

$x = 0$:

$$U_1^i - u^i(0) = 0 \quad \text{or} \quad S_1^i + N^i(0) = 0, \tag{29}$$

$$U_2 - w(0) = 0 \quad \text{or} \quad S_2 + Q(0) = 0, \tag{30}$$

$$U_3 - \varphi(0) = 0 \quad \text{or} \quad S_3 + M(0) = 0. \tag{31}$$

$x = L$:

$$U_4^i - u^i(L) = 0 \quad \text{or} \quad S_4^i - N^i(L) = 0, \tag{32}$$

$$U_5 - w(L) = 0 \quad \text{or} \quad S_5 - Q(L) = 0, \tag{33}$$

$$U_6 - \varphi(L) = 0 \quad \text{or} \quad S_6 - M(L) = 0, \tag{34}$$

where U_1^i, U_2, U_3, U_4^i, U_5, U_6 represent the generalized boundary displacements for the six degrees of freedom. The S_1^i, S_2, S_3, S_4^i, S_5, S_6 are the concentrated forces at the end of the element of the beam and $i = \{1, 2, \ldots, N\}$.

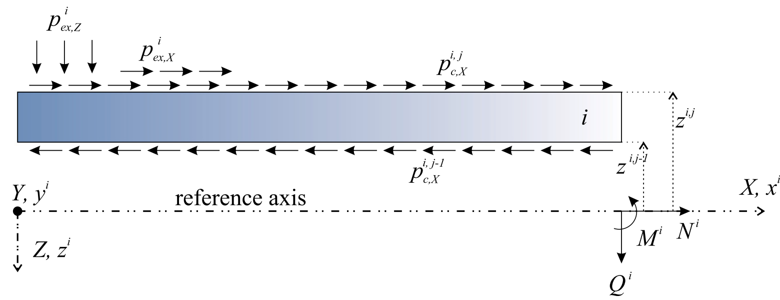

Fig. 3. Contact load acting on layer i, and equilibrium forces $N^i(x)$, $Q^i(x)$, $M^i(x)$ of layer i considered on the reference axis of the beam.

2.1. Modified principle of virtual work

The basic system of kinematic, equilibrium and constitutive equations is very complex to solve in general form, and the analytical solution is only possible if the model is somewhat simplified with a limited number of layers and a limited number of finger joints. The system of kinematic (13)–(15), equilibrium (17)–(19), and constitutive (24)–(26) equations can be solved numerically using the finite element method. For our numerical model, we used the finite elements based on the approximation of strains, first introduced by Planinc [36]. The formulation of finite elements is based on the principle of virtual work. The following derivation of finite elements is also based on the work of Čas [57], Schnabl [14], and Kroflič [5] with a modified application for multilayer composite beams. The basic formulation of the principle of virtual work essentially states that the work of the internal forces equals the work of the external loading on infinitesimally small virtual deformations and displacements [35,62]. When the composite beam consists of several layers, the virtual work of the beam is equal to the sum of the virtual work for all the layers and is written in general form as:

$$\begin{aligned}\delta W = \sum_{i=1}^{N} \delta W^i = \sum_{i=1}^{N} \Bigg(\int_0^L N^i \delta\varepsilon^i dx + \int_0^L Q \delta\gamma dx + \int_0^L M \delta\kappa dx - \\ - \int_0^L (p_X^i + p_{c,X}^{i,j} - p_{c,X}^{i,j-1}) \delta u^i - \int_0^L p_Z^i \delta w - \\ - \int_0^L m_Y^i \delta\varphi - \sum_{k=1}^{6} S_k^i \, \delta U_k^i \Bigg).\end{aligned} \tag{35}$$

The quantities δu^i, δw, and $\delta\varphi$ are virtual perturbations of the horizontal and vertical displacements and rotations of the reference axis x, and $\delta\varepsilon^i$, $\delta\gamma$, and $\delta\kappa$ are virtual perturbations of the axial and shear deformations and curvature of the layer i. The δU_1^i, δU_2, δU_3, δU_4^i, δU_5, δU_6 are virtual perturbations of generalized nodal kinematic quantities:

$$\begin{aligned} \delta U_1^i &= \delta u^i(0), & \delta U_4^i &= \delta u^i(L), \\ \delta U_2 &= \delta w(0), & \delta U_5 &= \delta w(L), \\ \delta U_3 &= \delta\varphi(0), & \delta U_6 &= \delta\varphi(L). \end{aligned} \tag{36}$$

Since it is assumed that the constitutive equations, Eqs. (24)–(26), are identically satisfied, the equilibrium forces and bending moments can be replaced by constitutive forces and bending moments, i.e., $N^i = N_C^i$, $Q = Q_C$, $M = M_C$. According to the kinematic equations, Eqs. (13)–(15), there are only three independent variables between u^i, w, φ, ε^i, γ, and κ. It has been shown that the finite element formulation using the kinematic quantities u^i, w, φ may exhibit locking and is not as robust as the formulation using the deformation variables ε^i, γ, and κ as unknowns [49]. For this reason, the finite element formulation used is referred to as a locking-free strain-based finite element formulation [35,36]. The problem is considered as a constrained variational calculus problem and the kinematic equations as the constraints of the problem. To introduce them into the principle of virtual work in Eq. (35), the kinematic equations, Eqs. ((13)–(15)), are multiplied by the Lagrangian multipliers R_1^i, R_2 and R_3. The multipliers can be chosen arbitrarily, but must be differentiable, i.e., continuous on $x \in [0, L^i]$. Since it is assumed that all layers have the same initial length, the products are then integrated over the length of the finite element L. As we proceed, the expressions are varied with respect to the unknown displacements and strains u^i, w, φ, ε^i, γ, κ, and the Lagrangian multipliers R_1^i, R_2, R_3. The expression with the first derivatives of displacements and strains is partially integrated and added to the principle of virtual work δW, Eq. (35). The final and simplified form of the functional *modified principle of virtual work* δW^{**} for a composite beam with interlayer slips is written as:

$$\begin{aligned}\delta W^{**} = \sum_{i=1}^{N} \Bigg\{ & \int_0^L \Big((N_C^i - R_1^i)\,\delta\varepsilon^i + (Q_C - R_2)\,\delta\gamma + (M_C - R_3)\,\kappa \Big) dx \\ & + \left(u^i(L) - u^i(0) - \int_0^L \varepsilon^i dx \right) \delta R_1^i \\ & + \left(w(L) - w(0) - \int_0^L (\gamma - \varphi) dx \right) \delta R_2 \\ & + \left(\varphi(L) - \varphi(0) - \int_0^L \kappa dx \right) \delta R_3 \\ & - \Big(R_1^i(0) + S_1^i \Big) \delta u^i(0) - \Big(R_2(0) + S_2 \Big) \delta w(0) \\ & - \Big(R_3(0) + S_3 \Big) \delta\varphi(0) \Bigg\} \\ & + \Big(R_1^i(L) - S_4^i \Big) \delta u^i(L) + \Big(R_2(L) - S_5 \Big) \delta w(L) \\ & + \Big(R_3(L) - S_6 \Big) \delta\varphi(L) = 0. \end{aligned} \tag{37}$$

This formulation expresses the modified principle of virtual work with only $N+2$ unknown functions $\varepsilon^i(x)$, $\gamma(x)$, and $\kappa(x)$. All other unknowns are represented by their boundary values $R_1^i(0)$, $R_2(0)$, $R_3(0)$, $R_1^i(L)$, $R_2(L)$, and $R_3(L)$, which are known and defined by the position of the element in N-layer composite beam. The basic equations are non-linear and generally cannot be solved in closed form, so a method involving approximation of the unknowns must be considered. The Petrov–Galerkin method is used to translate the complex continuous functions into smaller discrete functions that are easier to solve. At this point the assumptions defined by Eqs. (9)–(12) are used in the derivation of the initial Euler–Lagrange equations for the composite beam.

The element is divided into $N^\alpha - 1$ smaller sections with N^α nodes, where $\alpha = \{\varepsilon, \gamma, \kappa\}$. We assume that all layers have the same number of nodes, i.e., $N^{\varepsilon,i} = N^{\varepsilon,i+1} = N^\varepsilon$, $N^{\gamma,i} = N^{\gamma,i+1} = N^\gamma$, and $N^{\kappa,i} = N^{\kappa,i+1} = N^\kappa$. A Lagrange polynomial interpolation is used to approximate the unknown functions $\varepsilon^i(x)$, $\gamma(x)$, and $\kappa(x)$, although this is not a limitation of this method. The interpolation takes the form:

$$\varepsilon^i(x) \approx \sum_{n=1}^{N^\varepsilon} L_n(x)\,\varepsilon_n^i, \tag{38}$$

$$\gamma(x) \approx \sum_{n=1}^{N^\gamma} L_n(x)\,\gamma_n, \tag{39}$$

$$\kappa(x) \approx \sum_{n=1}^{N^\kappa} L_n(x)\,\kappa_n, \tag{40}$$

where the ε_n^i, γ_n, and κ_n are the discrete values of the axial, transverse and rotational strains determined at the nodes of the element and $i = \{1,2,\dots,N\}$. Similarly, the variations of the strains $\delta\varepsilon^i$, $\delta\gamma$, and $\delta\kappa$ are interpolated, see Eqs. (41)–(43), using the discrete nodal values $\delta\varepsilon_n^i$, $\delta\gamma_n$, and $\delta\kappa_n$. The collocation points for the variation are chosen to coincide with the nodal points.

$$\delta\varepsilon^i(x) \approx \sum_{n=1}^{N^\varepsilon} L_n(x)\,\delta\varepsilon_n^i, \tag{41}$$

$$\delta\gamma(x) \approx \sum_{n=1}^{N^\gamma} L_n(x)\,\delta\gamma_n, \tag{42}$$

$$\delta\kappa(x) \approx \sum_{n=1}^{N^\kappa} L_n(x)\,\delta\kappa_n. \tag{43}$$

The interpolations in Eqs. (38)–(43) are now substituted into the functional δW^{**} in Eq. (37). The fundamental lemma of the calculus of variations states that all coefficients associated with the independent variations in the functional must equal 0. In this way, the system of discrete generalized Euler–Lagrange equilibrium equations of the N-layer composite beam are obtained as follows:

$$f_{(i-1)N^\varepsilon+n} = \int_0^L (N_C^i - R_1^i)\,L_n(\xi)\,d\xi = 0; \qquad n = \{1,2,\dots,N^\varepsilon\}, \tag{44}$$

$$f_{N\cdot N^\varepsilon+n} = \int_0^L (Q_C - R_2)\,L_n(\xi)\,d\xi = 0; \qquad n = (1,2,\dots,N^\gamma\}, \tag{45}$$

$$f_{N\cdot N^\varepsilon+N^\gamma+n} = \int_0^L (M_C - R_3)\,L_n(\xi)\,d\xi = 0; \qquad n = \{1,2,\dots,N^\kappa\}, \tag{46}$$

$$f_{N\cdot N^\varepsilon+N^\gamma+N^\kappa+i} = u^i(L) - u^i(0) - \sum_{n=1}^{N^\varepsilon} L_n^*(x)\,\varepsilon_n^i dx = 0, \tag{47}$$

$$f_{N\cdot(N^\varepsilon+1)+N^\gamma+N^\kappa+1} = w(L) - w(0) + \varphi(0)\,L - \sum_{n=1}^{N^\gamma} L_n^*\gamma_n + \sum_{n=1}^{N^\kappa} L_n^{**}\,\kappa_n = 0, \tag{48}$$

$$f_{N\cdot(N^\varepsilon+1)+N^\gamma+N^\kappa+2} = \varphi(L) - \varphi(0) - \sum_{n=1}^{N^\kappa} L_n^*(x)\,\kappa_n dx = 0, \tag{49}$$

$$f_{N\cdot(N^\varepsilon+1)+N^\gamma+N^\kappa+2+i} = S_1^i + R_1^i(0) = 0, \tag{50}$$

$$f_{N\cdot(N^\varepsilon+2)+N^\gamma+N^\kappa+3} = S_2 + R_2(0) = 0, \tag{51}$$

$$f_{N\cdot(N^\varepsilon+2)+N^\gamma+N^\kappa+4} = S_3 + R_3(0) = 0, \tag{52}$$

$$f_{N\cdot(N^\varepsilon+2)+N^\gamma+N^\kappa+4+i} = S_4^i - R_1^i(0) - \int_0^L \left(p_X^i + p_{c,X}^{i,j} - p_{c,X}^{i,j-1}\right) dx = 0, \tag{53}$$

$$f_{N\cdot(N^\varepsilon+3)+N^\gamma+N^\kappa+5} = S_5 - R_2(0) - \sum_{i=1}^{N} \int_0^L p_Z^i dx = 0, \tag{54}$$

$$f_{N\cdot(N^\varepsilon+3)+N^\gamma+N^\kappa+6} = S_6 - R_3(0) - \int_0^L \left(R_2 - \sum_{i=1}^{N} m_Y^i\right) dx = 0, \tag{55}$$

where $i = (1,2,\dots,N)$, $j = (1,2,\dots,N-1)$ and $i = j$. The integrals of the Lagrangian polynomials are denoted by $L_n^*(x)$ and $L_n^{**}(x)$ and are:

$$L_n^*(x) = \int_0^x L_n(\xi)d\xi, \tag{56}$$

$$L_n^{**}(x) = \int_0^x \left(\int_0^\eta L_n(\xi)d\xi\right)d\eta, \tag{57}$$

for $x \in [0, L]$.

The finger joint is introduced into the model with additional equation:

$$f_{N(N^\varepsilon+3)+N^\gamma+N^\kappa+6+i} = u_{e_{\mathrm{FJ}}}^i(0) - u_{e_{\mathrm{FJ}}-1}^i(L_{e_{\mathrm{FJ}}-1}) - \frac{R_{1,e_{\mathrm{FJ}}}^i(0)}{K_{\mathrm{FJ}}}, \tag{58}$$

where $e_{\mathrm{FJ}} \in \{1,2,\dots,N_{el}\}$ is the index of the element in which the finger joint is located and $i \in \{1,2,\dots,N\}$ is the index of the layer where the finger joint is situated. N and N_{el} are the total number of layers and finite elements, respectively. In this way, the continuity of the kinematic field is ensured.

2.2. Solution of the discrete equations of a composite beam

The Eqs. (44)–(55) form the system of generalized equilibrium equations of a N-layer composite beam considering interlayer slip and the shear deformation of the layer while the presence of the finger joint in the axial direction represents a constraining equation that connects the two connecting elements at the level of the construction of the numerical model of the beam. Therefore, in general, the system consists of $n_g = N\,N^\varepsilon + N^\gamma + N^\kappa + 3\,N + 6$ algebraic equations for the same number of unknowns. The solution of the problem is obtained by solving the equation:

$$\mathbf{g}(\mathbf{u}) - \lambda\,\mathbf{p} = 0, \tag{59}$$

where $\mathbf{u}$ is the vector of the unknown components of the nodal displacements and rotations, i.e., external degrees of freedom, and $\mathbf{p}$ is the vector of the external load with load factor λ. For the numerical solution of Eq. (59), a well known Newton–Raphson iterative procedure was used, in which the Eqs. (44)–(55) must be linearized [59,60]. Thus, the tangent stiffness matrix $\mathbf{K_T}$ is obtained. If the determinant of the tangent stiffness matrix is 0, the Newton–Raphson method does not work and in the corresponding iteration the beam is considered to have failed and maximum stress is reached.

3. Numerical examples

3.1. Verification of the numerical model

The verification of the numerical model was carried out on the example of a four-layer, simply supported Euler–Bernoulli beam, taking into account interlayer slip. The length of the beam was 400 cm and the cross-section was $b = 10$ cm and $h = 28$ cm, as shown in Fig. 4. The results of the proposed numerical model were compared with those of Sousa and Silva [34] and Kroflič et al. [5], in which shear deformation was neglected. For our model, which takes into account the shear deformations of the layers, the shear modulus was considered to be very high, i.e. $G = 10^5$ kN/cm^2. The geometry and material properties were taken from Sousa and Silva [34], see Fig. 4. The beam was loaded with a uniformly distributed load $p_Z = 0.1$ kN/cm^2. The results of the four-layer beam are also verified with the analytical solution obtained using an analytical model similar to that of Fortuna et al. [63], but extended to the four layers. The results and comparisons for the interlayer slips at the left edge of the beam and for the vertical displacements at the midspan of the beam are given in Table 1 in numerical form for different numbers of elements N_{el} and different degrees of interpolation. For the calculations with the numerical model, the Lobatto interpolation method (L) was used. For example, the $2\,L_4$ means that the calculation with two finite elements was performed with the Lobatto interpolation method with fourth degree of interpolation. The results of the analytical model can also be found in Table 1. For each of the N_{el} the error of the numerical model is calculated in relation to the results of the analytical model and the results of Kroflič [5] and Sousa and Silva [34]. The error is calculated according to the simple expression: Error $= (s_{\mathrm{N}} - s_{\mathrm{M}})/s_{\mathrm{M}}\ 100\%)$, where s_{N} represents the numerical solution and s_{M} represents the reference solution, where letter M stands for reference solutions obtained by analytical model (M=A), Kroflič et al. [5] model

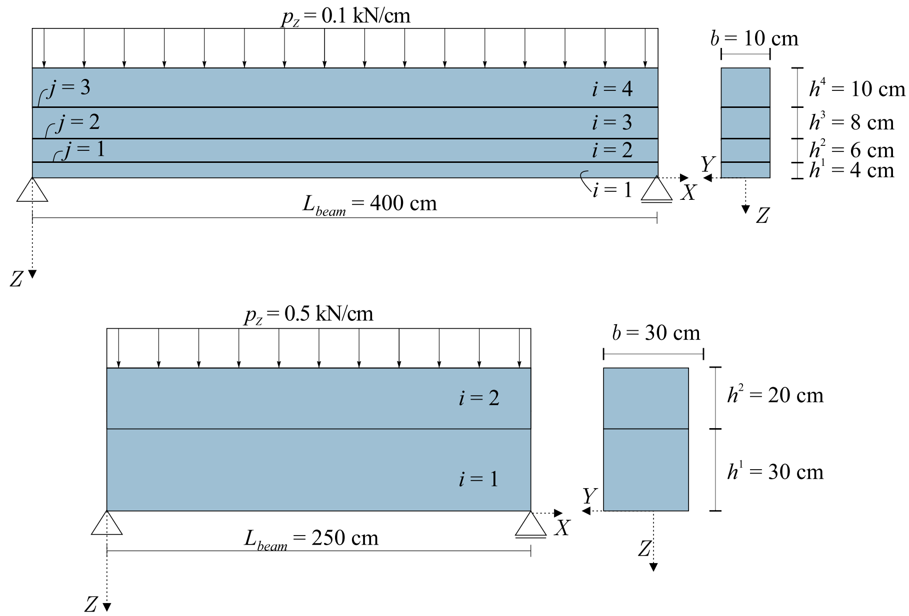

Fig. 4. The two models of a four- and two-layer, simply supported glued laminated beam with interlayer slip for the verification of the numerical model.

(M=K) or Sousa and Silva [34] model (M=S). When comparing with the literature, the numerical model presented agreed most with that of Sousa and Silva [34]. It can be seen that the majority of the results agree at least up to the 6th decimal place.

An additional verification of the numerical model was also carried out on the example of a two-layer Timoshenko–Ehrenfest composite beam analysed by Schnabl et al. [49], where the rotations φ^i, pseudocurvatures κ^i and shear strains γ^i are considered to be different for the layers i and where interlayer slip was also taken into account. The length of the beam was L = 250 cm with a cross-section of $b \times h$ = 30×50 cm. The bottom layer has a thickness of 30 cm and a shear modulus G = 120 kN/cm^2, while the top layer has a shear modulus of G = 80 kN/cm^2. The modulus of elasticity was the same for both layers, E = 1200 kN/cm^2. The beam was loaded with a uniform load p_Z = 0.5 kN/cm. The verification was done with finger joint at the midspan with very high stiffness ($K_{FJ} = 10^{15}$ kN/cm^2), so the results are comparable to those by Schnabl et al. [49], but not necessarily the same. The formulation by Schnabl et al. [49] is different than that presented in this paper because the vertical displacements, rotations and shear deformations were not considered to be the same for all layers as is the case in this formulation. Consequently, the results are slightly different, as can be seen in Table 1, where (N2) denotes the numerical solution for the two-layer beam and (S2) denotes the solution for the two-layer beam according to Schnabl [49].

For the example of four-layer beam the horizontal slips Δ_X^j of all three interlayer contacts $j = \{1, 2, 3\}$ are shown graphically in Fig. 5. The results of all three models presented agree well. A small deviation of the values can be seen for the lowest interlayer contact j = 1. This could be due to the fact that we assumed the same shear modulus G as Kroflič et al. [5] where delamination between layers was also considered and the author had to assume a high contact stiffness perpendicular to the layers, $K_Z \gg 0$. Since our model does not take delamination into account this assumption was not considered.

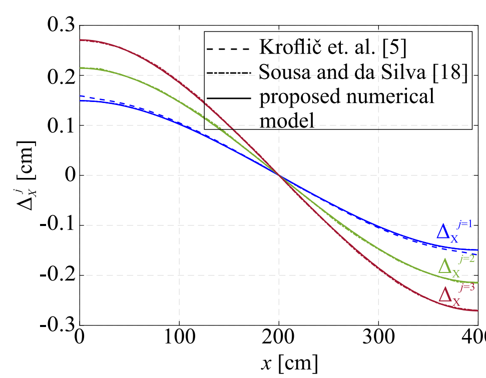

Fig. 5. The comparison of the interlayer slips Δ_X^j of the four-layer glued laminated beam calculated with the numerical model with the results from the literature [5,34].

3.2. Validation of the numerical model

In order to validate the results calculated with the presented numerical model, experimental tests were carried out. Four glued laminated beams were tested using a four-point bending test setup according to the requirements of the standard EN 408 [64]. The beams were made of Slovenian beech wood. The length of the beams was 360 cm. The cross-section of the beams was rectangular with a height h = 18 cm and a width b = 10 cm and each beam had 10 layers. The schematic representation of the beams can be found in Fig. 6. Three of the beams had finger joints in the bottom layer at the midspan region where the maximum bending moment occurs, while the bottom layer of Beam 1 was free of finger joints at the midspan. All the mechanical properties of the material of the glued laminated beams required for the numerical model were measured before testing and are shown in Table 2. The modulus of elasticity E_t^i of the layers denoted by i, where $i = \{1, 2, \ldots, 10\}$, was determined by nondestructive testing with the STIG strength grading machine, presented in the work of Fortuna et al. [3,65]. The shear modulus of the beam, G, was measured during the experimental bending test according to the EN 408 [64]. The stiffness of the interlayer contact, K_X, was also determined during the beam bending tests, while tensile tests for the finger joints were performed to determine the stiffness of the finger joints, K_{FJ}, needed as input data for the numerical model and its validation. The stiffness, K_{FJ}, was determined based on the measurements of the tensile modulus of elasticity of the finger joints, $E_{t,FJ}$. Since our model is a planar model where the finger joints are considered as axial springs, the stiffness of the finger joints is calculated here according to Eq. (60):

$$K_{FJ} = \frac{b\,h^i}{l_{FJ}\,E_{t,FJ}}. \tag{60}$$

Table 1
Interlayer slips Δ_X^j and vertical displacements at the midspan of the four-layer Timoshenko–Ehrenfest and two-layer Euler–Bernoulli beam, calculated with the proposed numerical models and their comparison with the analytical results [63] and other numerical models [5,34,49], where L_k denotes the Lobatto method and k the degree of interpolation.

Quantity	Description	Reference solution	Number of elements and type of interpolation				
			$2\,L_2$	$10\,L_2$	$12\,L_2$	$4\,L_3$	$2\,L_4$
[cm]		Four-layer beam (Fig. 4)					
Δ_X^1 (0)	Numerical model (N)		0.149203	0.149300	0.149301	0.149301	0.149301
	Analytical model (A) [63]	0.149301					
	Kroflič et. al. (K) [5]	0.158872					
	Sousa and Silva (S) [34]	0.149301					
	Error N vs. A [%]		0.0656	0.0067	0	0	0
	Error N vs. S [%]		0.0656	0.0067	0	0	0
	Error N vs. K [%]		6.0860	6.0250	6.0244	6.0244	6.0244
Δ_X^2 (0)	Numerical model (N)		0.214215	0.214333	0.214333	0.214333	0.214333
	Analytical model (A) [63]	0.214333					
	Kroflič et. al. (K) [5]	0.215143					
	Sousa and Silva (S) [34]	0.214333					
	Error N vs. A [%]		0.0551	0	0	0	0
	Error N vs. S [%]		0.0551	0	0	0	0
	Error N vs. K [%]		0.4313	0.37649	0.037649	0.037649	0.037649
Δ_X^3 (0)	Numerical model (N)		0.270728	0.270895	0.270896	0.270896	0.270896
	Analytical model (A) [63]	0.270896					
	Kroflič et. al. (K) [5]	0.269841					
	Sousa and Silva (S) [34]	0.270896					
	Error N vs. A [%]		0.0620	0.0004	0	0	0
	Error N vs. S [%]		0.0620	0.0004	0	0	0
	Error N vs. K [%]		−0.3287	−0.3906	−0.39097	−0.39097	−0.39097
w $(L/2)$	Numerical model (N)		3.831362	3.828018	3.828014	3.828014	3.828014
	Analytical model (A) [63]	3.828015					
	Kroflič et. al. (K) [5]	3.835192					
	Sousa and Silva (S) [34]	3.827935					
	Error N vs. A [%]		−0.0874	−0.0001	0	0	0
	Error N vs. S [%]		−0.0895	−0.00217	−0.0021	−0.021	−0.021
	Error N vs. K [%]		0.0999	0.1871	0.1872	1.872	1.872
			Two-layer beam				
Δ_X (0)	Numerical model (N2)		0.076541	0.076544	0.076544	0.076544	0.076544
	Schnabl et. al.(S2) [49]	0.077293					
	Error N2 vs. S2 [%]		−0.9725	−0.9692	−0.9692	−0.9692	−0.9692
w $(L/2)$	Numerical model (N2)		0.270066	0.270053	0.270053	0.270053	0.270053
	Schnabl et. al.(S2) [49]	0.271026					
	Error N2 vs. S2 [%]		−0.3543	−0.3592	−0.3592	−0.3592	−0.3592

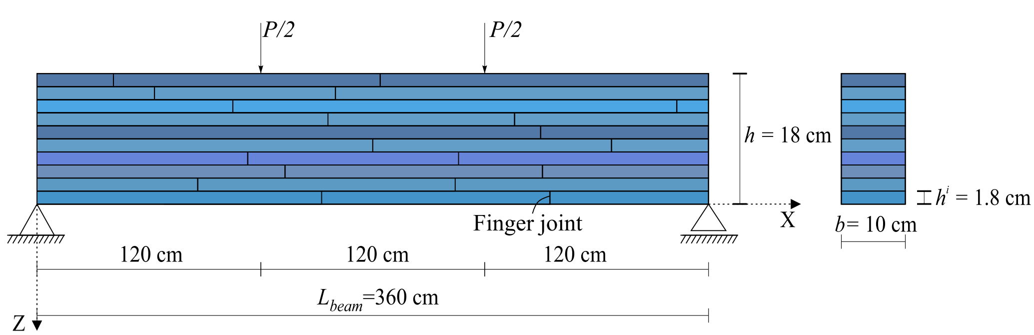

Fig. 6. One of the four simply supported ten-layer glued laminated beam with finger joints loaded with concentrated load and experimentally tested in bending.

The average value of the measured modulus of elasticity in tension of all finger joints, $E_{t,\mathrm{FJ}} = 1242$ kN/cm^2, was taken into account for each of the finger joints. Each layer had approximately two finger joints. The positions of the finger joints, x_{FJ}, were measured from the left edge of the beam and are given in Table 3 for each layer. This gave us all the input data we needed for the simulations with the numerical model.

During the experimental bending test, the applied load and the vertical displacements were monitored. The comparison between the experimentally measured and the numerically calculated responses of the four beams is shown with numerical values in Table 4 and graphically in Fig. 7. It can be observed that the measured and calculated results agree quite well. It should be noted that no type of adjustment or calibration was performed to obtain the results shown for Beams 2, 3 and 4. As can be seen from Fig. 7, these three beams show almost linear-elastic behaviour. However, this was not the case for Beam 1, i.e., the beam without finger joints in the bottom layer in the region of maximum bending moments, i.e., maximum bending stresses. From the experimentally measured responses for all beams, it appears that failure occurred at a load of about 80 kN, resulting in a limiting stress of $f_{lim} = 80$ kN/cm^2. Therefore, we adjusted the constitutive material law for Beam 1 so that the initial response was linear-elastic up to the bending stress f_{lim}. At higher stresses, the constitutive law became non-linear. The contact between the layers was also modelled as non-linear. Both constitutive laws are shown in Fig. 8. In this way we obtained the results shown in Fig. 7 for Beam 1 and the agreement of the results was increased (see Table 4).

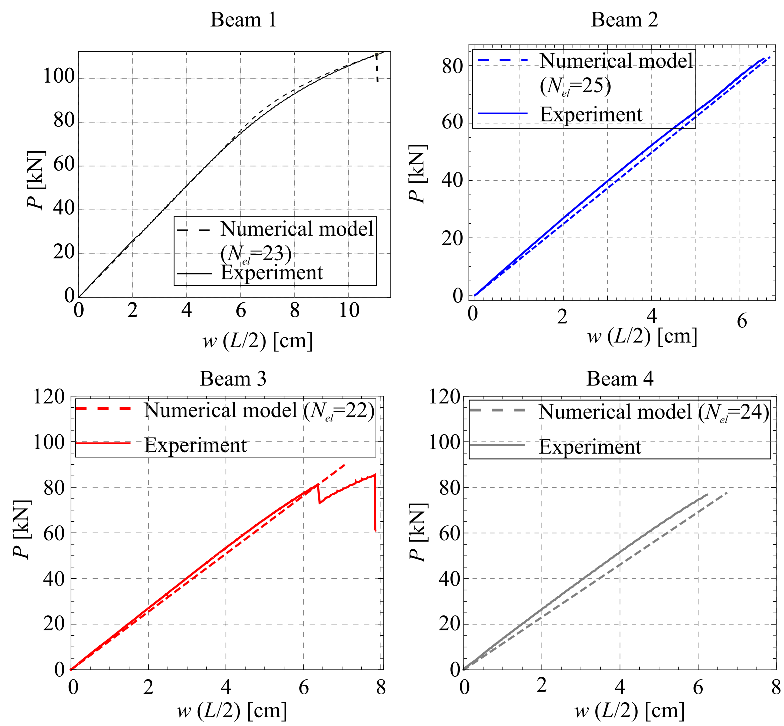

Fig. 7. The comparison of the results calculated with the numerical model (dashed line) and the results measured experimentally in bending tests (solid line) of the ten-layer glued laminated beam.

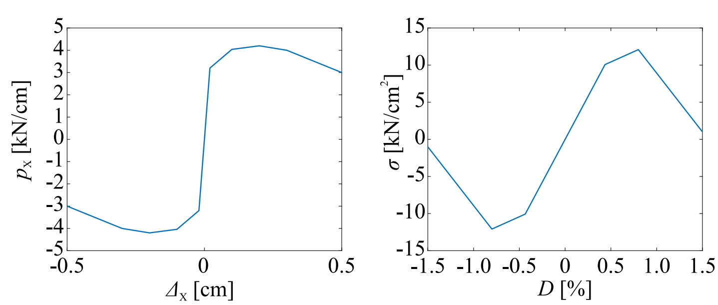

Fig. 8. Nonlinear constitutive law for the interlayer contact between the layers (left) and the non-linear constitutive law for the layers (right) as input data for non-linear numerical model of Beam 1.

3.3. Robustness of the numerical model

The results of the verification of the numerical model (Table 1) show that the output of the model is influenced by the number of finite elements (N_{el}) used in the model and the complexity of the interpolation, i.e., the degree of interpolation (d.o.i.). Thus, the robustness of the model is investigated in terms of convergence and the sensitivity of the model, i.e., the effect of the extreme values of the input data on the results of the model. As mentioned earlier, similar finite elements were presented by Schnabl et al. [49], where the performance of the finite elements of the two-layer Timoshenko–Ehrenfest beam was analysed. They showed rapid convergence of results and also no problems with shear or slip locking. The type of finite elements presented in this paper is somewhat more complex and has more layers with the presence of finger joints. However, in this formulation, it is assumed that the vertical displacements, rotations and shear deformations are the same for all layers. This could affect the robustness of the model. In this part, the influence of the number of elements N_{el}, the interpolation method and the degree of interpolation on the robustness of the finite elements is further investigated. Table 5 shows the convergence of the model of the ten-layer beam with a finger joint at the midspan. The geometry of the beam is similar to the one used for the validation of the model, with a length L = 360 cm, a width b = 10 cm and a height h = 18 cm (Fig. 9). The interlayer stiffness was K_X = 15 kN/cm^2. The material properties were the same for all ten layers, i.e., modulus of elasticity E = 1800 kN/cm^2 and shear modulus was G = 150 kN/cm^2. The results were obtained using two different methods to calculate the interpolation points: Equidistant (E) and Lobatto (L) method. As can be seen from the derivation of our numerical model, the finger joints determine the meshing of the model, so for one finger joint in the model at least two finite elements are needed (N_{el} = 2). The results are shown for different d.o.i. of Lagrangian polynomials to approximate of the unknown quantities and then compared with the reference solution calculated with 100 finite elements of the same length. The method of interpolation and integration for the reference solution was not significant, as the results for both methods were identical up to the seventh significant figure. As can be seen in Table 5, the convergence of the results depends on the stiffness of the finger joint. If the stiffness of the finger joint is very high (K_{FJ} = 10^{15} kN/cm^2), we were able to obtain the correct results in bold already with only two finite elements, while for a very low stiffness of the finger joints (K_{FJ} = 10^{-3} kN/cm^2) more finite elements with a higher degree of interpolation (d.o.i.) were needed. Interpolation with Lobatto points gives slightly better results than those with Equidistant points.

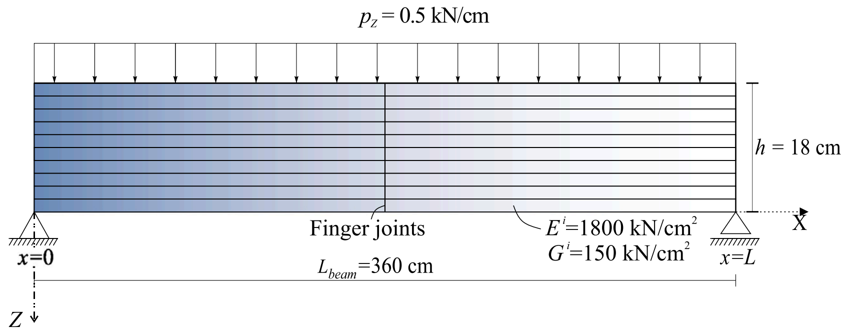

Fig. 9. Model of a simply supported ten-layer glued laminated beam with finger joints at the midspan loaded with uniform distributed load.

Table 2
Mechanical properties of the laminations of the glued laminated beams as input data for the numerical models of the four glued laminated beams experimentally tested in bending.

Property	Mechanical properties [kN/cm]^2			
	Beam 1	Beam 2	Beam 3	Beam 4
E_t^{10}	18 500	20 800	17 500	17 100
E_t^{9}	18 000	17 800	20 200	17 000
E_t^{8}	18 800	20 300	19 400	18 500
E_t^{7}	14 400	17 300	20 300	18 900
E_t^{6}	19 300	16 600	19 000	22 100
E_t^{5}	16 300	17 600	14 900	21 200
E_t^{4}	19 200	20 300	18 100	17 900
E_t^{3}	19 700	15 200	20 200	18 700
E_t^{2}	20 600	18 100	20 000	18 100
E_t^{1}	21 000	21 100	20 700	20 700
G	64.0	62.0	94.0	98.0
K_X	160.0	157.0	243.0	156.0
K_{FJ}	5590	5590	5590	5590

Table 3
Positions of the finger joints x_{FJ}^i for layers $i = (1, 2, \dots, 10)$ measured from the left edge of the beam as an input data for the numerical models of the four glued laminated beams experimentally tested in bending.

Property	Positions of finger joints [cm]			
	Beam 1	Beam 2	Beam 3	Beam 4
x_{FJ}^{10}	165	41, 184	57, 186	34, 190
x_{FJ}^{9}	186	63, 160	30, 342	159
x_{FJ}^{8}	111, 239	105, 343	136, 279	90
x_{FJ}^{7}	174, 341	156, 256	81, 223	19, 162
x_{FJ}^{6}	111, 287	270, 358	50, 192, 306	127, 254
x_{FJ}^{5}	296	180, 308	165	79
x_{FJ}^{4}	97	113, 226	104, 232	38, 166, 294
x_{FJ}^{3}	347	133, 271	140, 232	171, 267
x_{FJ}^{2}	351	87, 225	192	129, 283
x_{FJ}^{1}	301	68, 275	165, 307	132, 275

If one compares the results with those in the work of Schnabl et al. [49], it can be seen that in our case the convergence is somewhat slower. Therefore, an additional verification was made for the same model of a two-layer beam as reported by Schnabl et al. [14]. The results, presented in Table 6, show that the reference solution is already reached with the 3rd degree Lobatto interpolation, which is faster compared to the results of the model of the ten-layer beam. Thus, the complexity of the model (especially in terms of the number of layers) could be considered as one of the factors affecting the convergence of the results. Nevertheless, the results have shown that accurate results can be obtained with a small number of finite elements and a relatively low degree of interpolation. This leads to fast and efficient calculations.

Table 4
Values measured experimentally in bending tests and values calculated with the numerical model for the maximum vertical displacements at the midspan of the glued laminated beams with finger joints.

Specimen	N_{el}	Numerical (N) $w^N(L/2)$ [cm]	Measured (M) $w^M(L/2)$ [cm]	Error [%] $\frac{w^N(L/2)-w^M(L/2)}{w^M(L/2)}100$
Beam 1 (linear)	17	9.53	11.55	17.5
Beam 2 (linear)	24	6.96	6.92	−0.6
Beam 3 (linear)	22	7.05	7.85	10.2
Beam 4 (linear)	24	6.72	6.23	−7.9
Beam 1 (non-linear)	25	11.1	11.55	−4.3

Another important advantage of the presented finite element formulation is that finite elements do not exhibit problems regarding slip locking. This is demonstrated using the example of simply supported ten-layer beam, as shown in Fig. 9, with one finger joint in each layer positioned at the midspan of the beam. The results are shown in Fig. 10, where the interlayer slip between the lowest two layers is shown for two cases with very low interlayer contact stiffness (K_X = $1.5 \cdot 10^{-3}$ kN/cm^2) and very high interlayer contact stiffness (K_X = $1.5 \cdot 10^3$ kN/cm^2) using different methods of interpolation. Theoretically, slip locking occurs at the extreme values of the interlayer contact stiffness. Since Fig. 10 shows that the results remain stable regardless of the value of the stiffness K_X, it is proven that the finite elements are not subject to the slip locking problem.

3.4. Parametric study

3.4.1. Influence of the shear modulus G

With the present model we can evaluate the influence of shear modulus G on the response of a multilayer beam with interlayer slip. In the first parametric study, the vertical displacements at the midspan of the beam are analysed for different values of the shear modulus G of the ten-layer simply supported beam with the geometry already shown in Fig. 9. The contact stiffness between the layers was assumed to be $K_X = 150$ kN/cm^2. The vertical displacements at midspan $w(L/2)$ are plotted for four different shear moduli G, as shown in Fig. 11. The results of the numerical model are as expected, for larger shear modulus, the vertical displacements are smaller. For a very small value of shear modulus $G = 1.5$ kN/cm^2, the vertical displacement was almost 3.5 times larger than the vertical displacement for the case with a very large value of shear modulus $G = 15 \cdot 10^4$ kN/cm^2. These values of shear modulus are quite extreme values and were analysed to investigate the sensitivity of the model to the shear locking problems. Since the results are stable and show no oscillations, it can be concluded that the finite elements are free from shear locking.

Table 5
Comparison of numerical results for two and four elements with different degrees (d.o.i.) and types (t.o.i.) of interpolation to the reference solution obtained with 100 elements and 10th degree of for the slip in the lower interlayer contact at the beginning of the ten-layer beam and vertical displacement at the midspan of the ten-layer beam with finger joint at the midspan of each layer.

N_{el}	d.o.i.	t.o.i.	$w(L/2)$ [cm]	$\Delta^1_X(0)$ [cm]	Error $w(L/2)$ [%]	Error $\Delta_X(0)$ [%]
$K_{FJ} = 10^{15}$						
2	3	L	32.31938	−0.190808	−0.05	−4.03
		E	32.31461	−0.189477	−0.06	−4.70
2	4	L	32.33837	−0.196388	0.01	−1.22
		E	32.34325	−0.194721	0.03	−2.06
2	6	L	32.33451	−0.198707	0	−0.06
		E	32.33562	−0.198107	0	−0.36
2	10	L	**32.33436**	**−0.198819**	0	0
		E	32.33439	−0.198807	0	−0.01
4	3	L	32.33437	−0.197501	0	−0.66
		E	32.33435	−0.196978	0	−0.93
4	4	L	**32.33436**	−0.198648	0	−0.09
		E	32.33437	−0.198329	0	−0.25
4	5	L	**32.33436**	−0.198804	0	−0.01
		E	**32.33436**	−0.198696	0	−0.06
4	10	L	**32.33436**	**−0.198819**	0	0
		E	**32.33436**	**−0.198819**	0	0
Reference solution			**32.33436**	**−0.198819**	/	/
$K_{FJ} = 10^{3}$						
2	5	L	34.78062	−0.197979	0.01	−0.23
		E	34.78686	−0.197203	0.03	−0.62
2	6	L	34.77792	−0.198304	0	−0.07
		E	34.78441	−0.197508	0.02	−0.47
2	10	L	**34.77682**	**−0.198439**	0	0
		E	34.77696	−0.198422	0	−0.01
Reference solution			**34.77682**	**−0.198439**	/	/
$K_{FJ} = 10^{-3}$						
2	5	L	250.3163	−0.220419	1.77	4.60
		E	259.2459	−0.251162	5.40	19.2
2	6	L	246.7966	−0.208846	0.34	−0.89
		E	251.3316	−0.192304	2.18	−8.74
2	10	L	245.9662	**−0.210717**	0	0
		E	**245.9660**	−0.210719	−0.01	0.001
4	10	L	**245.9660**	**−0.210717**	0	0
Reference solution			**245.9660**	**−0.210717**	/	/

Table 6
Comparison of numerical results of the model of two-layer beam with interlayer slip for two elements with different degrees (d.o.i.) and types (t.o.i.) of interpolation to the reference solution given by Schnabl et. al. [49] for the slip at the beginning of the ten-layer beam and vertical displacement at the midspan of the two-layer beam.

N_{el}	d.o.i.	t.o.i	$w(L/2)$ [cm]	$\Delta^1_X(0)$ [cm]	Error $w(L/2)$ [%]	Error $\Delta^1_X(0)$ [%]
2	2	L	0.270066	−0.076541	0.005	−0.003
		E	0.270066	−0.076541	0.005	−0.003
2	3	L	**0.270053**	**−0.076544**	0	0
		E	0.270051	−0.076543	−0.001	−0.001
2	4	L	**0.270053**	**−0.076544**	0	0
		E	**0.270053**	**−0.076544**	0	0
2	5	L	**0.270053**	**−0.076544**	0	0
		E	**0.270053**	**−0.076544**	0	0
Ref. sol. (Schnabl et. al. [49])			**0.270053**	**−0.076544**	/	/

3.4.2. Influence of the number of layers and the interlayer contact stiffness

The study on the influence of the number of layers was carried out on the model of a simply supported glued laminated beam with the cross-section $b \times h = 20 \times 30$ cm. The length of the beam was $L = 400$ cm. The modulus of elasticity was assumed to be $E_t = 1760$ kN/cm^2 and the shear modulus was assumed to be $G = 80$ kN/cm^2 for all layers. In this case, the model had no finger joints. The number of layers varied between 2 and 10. In all cases, the total height of the beam remained the same ($h = 30$ cm) and the thickness of all layers was the same, so increasing the number of layers resulted in thinner layers. For the parametric study, three different contact stiffness between the layers were considered: $K_X = 50{,}100$ and 150 kN/cm^2. The Fig. 12 shows the results for the interlayer slip in the lowest interlayer contact at the end of the beam ($\Delta_X^{j=1}(L_{beam})$). As the number of layers is increased, the interlayer slip decreases. Intuitively, this means that the interlayer slip becomes smaller when stiffness of the interlayer contact is increased.

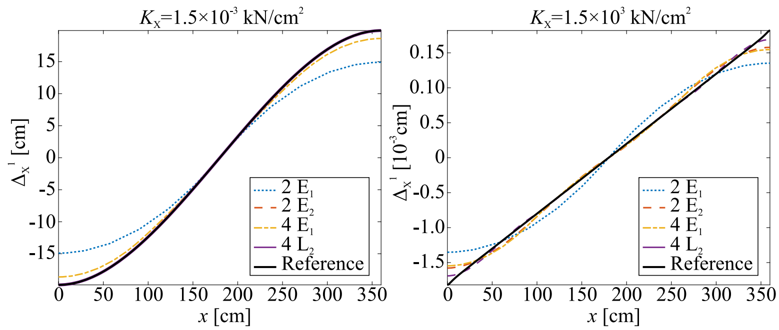

Fig. 10. Interlayer slip between the lower two layers along the length of a simply supported ten-layer beam with interlayer slip and finger joints at the midspan of the beam for two different interlayer contact stiffness K_X.

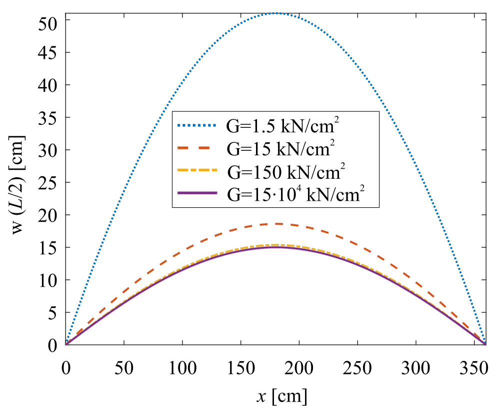

Fig. 11. Vertical displacement at the midspan of the ten-layer beam with interlayer slip and finger joints at the midspan in all layers for four different values of the shear modulus G of the layers.

The influence of the number of layers is more pronounced when the contact stiffness between the layers is lower. Similar conclusions can be drawn also for the vertical displacement at the midspan of the beam $w(L/2)$. When the contact stiffness between the layers is lower, the vertical displacement increases. This effect is more pronounced when the number of layers is larger.

3.4.3. Influence of the finger joint stiffness

The influence of the finger joint stiffness was investigated on the ten-layer glued laminated beam with a length of $L = 360$ cm and a prismatic cross-section. The geometry of the beam is similar to that already shown in Fig. 6. In each of the lowest three layers of the Beam 2 there were two finger joints with the same positions x^i_{FJ}, for $i = \{1, 2, 3\}$, while the upper seven layers were considered to be finger joint free. As can be seen from Fig. 13, the influence of finger joint stiffness is not very pronounced. It is shown together with the influence of the material modulus of elasticity in tension E_t. The stiffness of the finger joint is recalculated here according to Eq. (60) and presented with the modulus of elasticity of the finger joints $E_{t,\mathrm{FJ}}$ in order to be comparable with the modulus of elasticity of the layers E_t.

The influence of E_t gives a better overview of the influence of finger joint stiffness, which is relatively small, although Fortuna et al. [63] have shown that the influence of finger joint stiffness is very pronounced for two-layer Euler–Bernoulli glued laminated beams. In this case, however, we are dealing with a ten-layer beam where the finger joint stiffness is not as important as in the two-layer beams. The vertical displacement at the midspan of the beam depends mainly on the stiffness of the material and the stiffness of the interlayer contact K_X.

4. Conclusions

The formulation of a new type of finite element for the numerical analysis of N-layer composite beams with interlayer sliding is presented, taking into account the shear deformation of the layers and finger joints in the layers. The derivation of the finite element is based on a planar beam theory for an arbitrary number of layers. For the formulation of the strain-based finite elements, the modified principle of virtual work was adopted. Based on the results of our research presented in this work following conclusions can be drawn:

- Strain-based finite elements has proven to be a very effective and robust type of finite element also for modelling N-layer composite beams with finger joints.
- The analysis of different configurations of composite beams showed the applicability of the finite elements. The numerical model was validated with the results of experimental testing of four ten-layer glued laminated beams. Without any kind of calibration, the results of the numerical models agreed very well with the results of the bending tests.
- The numerical model of the four-layer glued laminated beam, which takes into account the interlayer slip, was verified by comparing the results with those from the literature and with the analytical solution. Again, the differences between the results were minimal and were considered to be due to different assumptions or simplifications of the models, such as neglecting shear deformations or delaminations, etc.
- Analysis of the convergence of the finite elements showed that we were able to obtain accurate solutions with a small number of elements and a relatively low degree of interpolation. The two methods for calculating the interpolation points, the Equidistant and the Lobatto points, are compared. It is found that the convergence of the results with the Lobatto points is slightly better, but the difference is very small.
- It was found that the convergence depends also on the complexity of the model, i.e., the number of layers, the interlayer contact stiffness and the stiffness of the finger joints.
- The performance of the finite elements was very stable and no slip or shear locking was observed in our analysis, as the results were stable and did not oscillate.

Thus, the presented finite elements are a practical tool for fast and accurate calculations for use in various numerous applications in numerical modelling of composite beams.

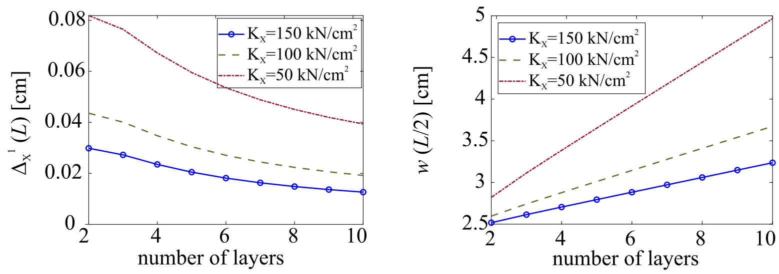

Fig. 12. Dependence of the interlayer slip at the and of the beam (left) and vertical displacement at the midspan of the beam (right) on the number of layers.

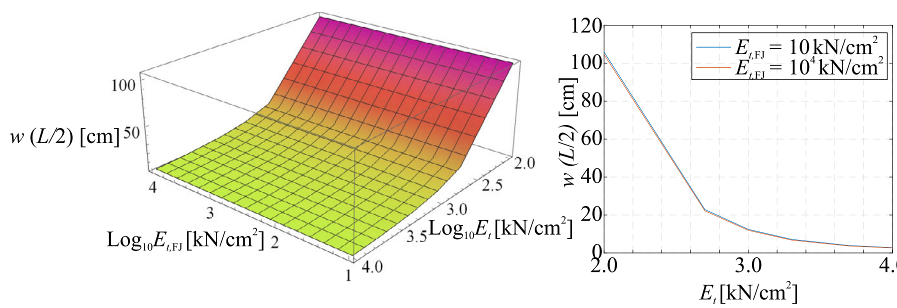

Fig. 13. Influence of the moduli of elasticity in tension of the layers, E_t, and of the finger joints $E_{t,\mathrm{FJ}}$, on the vertical displacement at the midspan $w(L/2)$ of the ten-layer beam.

CRediT authorship contribution statement

Barbara Fortuna: Conception and design of study, Acquisition of data, Analysis and/or interpretation of data, Writing – original draft. **Goran Turk:** Conception and design of study, Acquisition of data, Analysis and/or interpretation of data, Writing – review & editing. **Simon Schnabl:** Conception and design of study, Analysis and/or interpretation of data, Writing – review & editing.

Declaration of competing interest

The authors declare that they have no known competing financial interests or personal relationships that could have appeared to influence the work reported in this paper.

Data availability

Data will be made available on request.

Acknowledgements

The authors gratefully acknowledge the financial support of the research from the Slovenian Research Agency for the funding within the research core No. P2-0260.

References

[1] N.M. Newmark, Test and analysis of composite beams with incomplete interaction, Proc. Soc. Exp. Stress Anal. 9 (1) (1951) 75–92.
[2] J.R. Goodman, E.P. Popov, Layered beam systems with interlayer slip, J. Struct. Div. 94 (1968) 2535–2548.
[3] B. Fortuna, B. Azinović, M. Plos, T. Šuligoj, G. Turk, Tension strength capacity of finger joined beech lamellas, Eur. J. Wood Wood Prod. 78 (5) (2020) 985–994.
[4] M. Khelifa, A. Celzard, M. Oudjene, J. Ruelle, Experimental and numerical analysis of CFRP-strengthened finger-jointed timber beams, Int. J. Adhes. Adhes. 68 (2016) 283–297.
[5] A. Kroflič, M. Saje, I. Planinc, Non-linear analysis of two-layer beams with interlayer slip and uplift, Comput. Struct. 89 (23) (2011) 2414–2424, http://dx.doi.org/10.1016/j.compstruc.2011.06.007.
[6] B. Čas, M. Saje, I. Planinc, Non-linear finite element analysis of composite planar frames with an interlayer slip, Comput. Struct. 82 (23) (2004) 1901–1912, http://dx.doi.org/10.1016/j.compstruc.2004.03.070.
[7] T. Hozjan, M. Saje, S. Srpčič, I. Planinc, Geometrically and materially non-linear analysis of planar composite structures with an interlayer slip, Comput. Struct. 114–115 (2013) 1–17, http://dx.doi.org/10.1016/j.compstruc.2012.09.012.
[8] D. Lolić, D. Zupan, M. Brojan, A consistent finite element formulation for laminated composites with nonlinear interlaminar constitutive law, Compos. Struct. 247 (2020) 112445.
[9] C. Adam, T. Furtmüller, Moderately large deflections of composite beams with interlayer slip, in: Contributions to Advanced Dynamics and Continuum Mechanics, Springer, 2019, pp. 1–17.
[10] C. Adam, T. Furtmüller, Flexural vibrations of geometrically nonlinear composite beams with interlayer slip, Acta Mech. 231 (1) (2020) 251–271.
[11] U.A. Girhammar, V.K.A. Gopu, Composite beam-columns with interlayer slip—exact analysis, J. Struct. Eng. 119 (4) (1993) 1265–1282.
[12] R. Xu, Y.-F. Wu, Analytical study of beams strengthened by adhesively bonded reinforcement with variable properties using state space method, Compos. Sci. Technol. 69 (11–12) (2009) 1912–1918, http://dx.doi.org/10.1016/j.compscitech.2009.04.011.
[13] P. Wu, D. Zhou, W. Liu, 2-D elasticity solutions of two-layer composite beams with an arbitrarily shaped interface, Appl. Math. Model. 40 (2) (2016) 1477–1493.
[14] S. Schnabl, Analiza ObnaŠanja Kompozitnih Nosilcev Pri Požaru (Ph.D. thesis), University of Ljubljana, Ljubljana, 2007.
[15] S. Schnabl, I. Planinc, The effect of transverse shear deformation on the buckling of two-layer composite columns with interlayer slip, Int. J. Non-Linear Mech. 46 (3) (2011) 543–553.
[16] R. Xu, G. Wang, Bending solutions of the Timoshenko partial-interaction composite beams using Euler-Bernoulli solutions, J. Eng. Mech. 139 (12) (2013) 1881–1885, http://dx.doi.org/10.1061/(ASCE)EM.1943-7889.0000614.
[17] I. Ecsedi, A. Baksa, Analytical solution for layered composite beams with partial shear interaction based on Timoshenko beam theory, Eng. Struct. 115 (2016) 107–117, http://dx.doi.org/10.1016/j.engstruct.2016.02.034.
[18] A.F. Siciliano, L. Škec, G. Jelenić, Closed-form solutions for modelling the rotational stiffness of continuous and discontinuous compliant interfaces in two-layer Timoshenko beams, Acta Mech. 232 (7) (2021) 2793–2824, http://dx.doi.org/10.1007/s00707-021-02958-x.
[19] L. Škec, G. Jelenić, Analysis of a geometrically exact multi-layer beam with a rigid interlayer connection, Acta Mech. 225 (2014) 523–541, http://dx.doi.org/10.1007/s00707-013-0972-5.
[20] M. Levinson, A new rectangular beam theory, J. Sound Vib. 74 (1) (1981) 81–87, http://dx.doi.org/10.1016/0022-460X(81)90493-4.
[21] J.N. Reddy, A simple higher-order theory for laminated composite plates, J. Appl. Mech. 51 (1984) 745–752.
[22] J. Reddy, On locking-free shear deformable beam finite elements, Comput. Methods Appl. Mech. Engrg. 149 (1) (1997) 113–132, http://dx.doi.org/10.1016/S0045-7825(97)00075-3, Containing papers presented at the Symposium on Advances in Computational Mechanics.
[23] E. Carrera, Historical review of zig-zag theories for multilayered plates and shells, Appl. Mech. Rev. 56 (3) (2003) 287–308, http://dx.doi.org/10.1115/1.1557614.

[24] E. Carrera, M. Filippi, P.K. Mahato, A. Pagani, One-dimensional CUF models for the analysis of laminated structures, in: 8th Australasian Congress on Applied Mechanics, ACAM 2014, As Part of Engineers Australia Convention 2014, 2014, pp. 95–102.

[25] M. Cinefra, Non-conventional 1D and 2D finite elements based on CUF for the analysis of non-orthogonal geometries, Eur. J. Mech. A Solids 88 (2021) 104273, http://dx.doi.org/10.1016/j.euromechsol.2021.104273.

[26] X. Lin, Y. Zhang, A novel one-dimensional two-node shear-flexible layered composite beam element, Finite Elem. Anal. Des. 47 (7) (2011) 676–682, http://dx.doi.org/10.1016/j.finel.2011.01.010.

[27] A. Pagani, A. de Miguel, M. Petrolo, E. Carrera, Analysis of laminated beams via unified formulation and Legendre polynomial expansions, Compos. Struct. 156 (2016) http://dx.doi.org/10.1016/j.compstruct.2016.01.095.

[28] A. Pagani, E. Carrera, Large-deflection and post-buckling analyses of laminated composite beams by carrera unified formulation, Compos. Struct. 170 (2017) 40–52, http://dx.doi.org/10.1016/j.compstruct.2017.03.008.

[29] N. Challamel, U.A. Girhammar, Lateral-torsional buckling of vertically layered composite beams with interlayer slip under uniform moment, Eng. Struct. 34 (2012) 505–513.

[30] N. Challamel, U.A. Girhammar, Lateral-torsional buckling of partially composite horizontally layered or sandwich-type beams under uniform moment, J. Eng. Mech. 139 (8) (2013) 1047–1064, http://dx.doi.org/10.1061/(ASCE)EM.1943-7889.0000489.

[31] B. Čas, I. Planinc, S. Schnabl, Analytical solution of three-dimensional two-layer composite beam with interlayer slips, Eng. Struct. 173 (2018) 269–282.

[32] S. Schnabl, I. Planinc, M. Saje, G. Turk, An analytical model of layered continuous beams with partial interaction, Struct. Eng. Mech. (3) (2006) 263–278.

[33] U.A. Girhammar, A simplified analysis method for composite beams with interlayer slip, Int. J. Mech. Sci. 51 (7) (2009) 515–530.

[34] J. Sousa, A. Silva, Analytical and numerical analysis of multilayered beams with interlayer slip, Eng. Struct. 32 (2010) 1671–1680, http://dx.doi.org/10.1016/j.engstruct.2010.02.015.

[35] M. Saje, I. Planinc, G. Turk, B. Vratanar, A kinematically exact finite element formulation of planar elastic-plastic frames, Comput. Methods Appl. Mech. Eng. 144 (1997) 125–151.

[36] I. Planinc, M. Saje, A quadratically convergent algorithm for the computation of stability points: The application of the determinant of the tangent stiffness matrix, Comput. Methods Appl. Mech. Engrg. 169 (1) (1999) 89–105, http://dx.doi.org/10.1016/S0045-7825(98)00178-9.

[37] L. Galuppi, G. Royer-Carfagni, Laminated beams with viscoelastic interlayer, Int. J. Solids Struct. 49 (18) (2012) 2637–2645.

[38] P. Wu, D. Zhou, W. Liu, L. Wan, D. Liu, Elasticity solution of two-layer beam with a viscoelastic interlayer considering memory effect, Int. J. Solids Struct. 94 (2016) 76–86.

[39] CEN, Timber Structures – Glued Laminated Timber and Glued Solid Timber – Requirements, European Committee for Standardization, 2013, (In English language).

[40] J. Ehlbeck, F. Colling, R. Görlacher, Einflußkeilgezinkter lamellen auf die biegefestigkeit von brettschichtholzträgern-entwicklung eines rechenmodells, Holz Als Roh-Und Werkstoff 43 (8) (1985) 333–337.

[41] J. Ehlbeck, F. Colling, R. Görlacher, Einflußkeilgezinkter lamellen auf die biegefestigkeit von brettschichtholzträgern-eingangsdaten für das rechenmodell, Holz Als Roh-Und Werkstoff 43 (8) (1985) 369–373.

[42] J. Ehlbeck, F. Colling, R. Görlacher, Einflußkeilgezinkter lamellen auf die biegefestigkeit von brettschichtholzträgern-überprüfung des rechenmodells mit hilfe von trägerversuchen, Holz Als Roh-Und Werkstoff 43 (8) (1985) 439–442.

[43] R. Foschi, J. Barrett, Glued-laminated beam strength: A model, J. Struct. Div. 106 (1980) 1735–1754.

[44] A. Yasunori, H. Sumio, T. Kajita, Elastic-plastic analysis of composite beams with incomplete interaction by finite element method, Comput. Struct. 14 (5–6) (1981) 453–462, http://dx.doi.org/10.1016/0045-7949(81)90065-1.

[45] B.J. Daniels, M. Crisinel, Composite slab behavior and strength analysis, part I: Calculation procedure, J. Struct. Eng. 119 (1) (1993) 16–35.

[46] A. Dall'Asta, A. Zona, Non-linear analysis of composite beams by a displacement approach, Comput. Struct. 80 (27–30) (2002) 2217–2228.

[47] R.E. Erkmen, M.A. Bradford, Ellimination of slip-locking in composite beam-column analysis by using the element–free Galerkin method, Comput. Mech. 46 (2011) 911–924.

[48] R.E. Erkmen, M.A. Bradford, Treatment of slip locking for displacement-based finite element analysis of composite beam–columns, Internat. J. Numer. Methods Engrg. 85 (7) (2011) 805–826.

[49] S. Schnabl, M. Saje, G. Turk, I. Planinc, Locking–free two–layer Timoshenko beam element with interlayer slip, Finite Elem. Anal. Des. 43 (9) (2007) 705–714, http://dx.doi.org/10.1016/j.finel.2007.03.002.

[50] X. Lin, Y. Zhang, P. Pathak, 2 - finite element analysis of beams, in: X. Lin, Y. Zhang, P. Pathak (Eds.), Nonlinear Finite Element Analysis of Composite and Reinforced Concrete Beams, in: Woodhead Publishing Series in Civil and Structural Engineering, Woodhead Publishing, 2020, pp. 9–27, http://dx.doi.org/10.1016/B978-0-12-816899-8.00002-X.

[51] O.C. Zienkiewicz, R.L. Taylor, J.M. Too, Reduced integration technique in general analysis of plates and shells, Internat. J. Numer. Methods Engrg. 3 (2) (1971) 275–290, http://dx.doi.org/10.1002/nme.1620030211.

[52] M. Crisfield, A quadratic mindlin element using shear constraints, Comput. Struct. 18 (5) (1984) 833–852, http://dx.doi.org/10.1016/0045-7949(84)90030-0.

[53] E.N. Dvorkin, K.-J. Bathe, A continuum mechanics based four-node shell element for general non-linear analysis, Eng. Comput. 1 (1984) 77–88.

[54] T.H.H. Pian, Derivation of element stiffness matrices by assumed stress distributions, AIAA J. 2 (7) (1964) 1333–1336, http://dx.doi.org/10.2514/3.2546.

[55] E. Carrera, A.G. de Miguel, A. Pagani, Extension of MITC to higher-order beam models and shear locking analysis for compact, thin-walled, and composite structures, Internat. J. Numer. Methods Engrg. 112 (13) (2017) 1889–1908, http://dx.doi.org/10.1002/nme.5588.

[56] E. Reissner, On one-dimensional finite-strain beam theory: The plane problem, J. Appl. Math. Phys. (ZAMP) 23 (1972) 795–804, http://dx.doi.org/10.1007/BF01602645.

[57] B. Čas, M. Saje, I. Planinc, Non-linear finite element analysis of composite planar frames with an interlayer slip, Comput. Struct. 82 (23) (2004) 1901–1912, http://dx.doi.org/10.1016/j.compstruc.2004.03.070, Computational Structures Technology.

[58] U. Rodman, Analiza nosilnosti prostorskih okvirnih konstrukcij z upoštevanjem materialnih in geometrijskih nepopolnosti (Ph.D. thesis), University of Ljubljana, Ljubljana, 2009.

[59] T. Hughes, K. Pister, Consistent linearization in mechanics of solids and structures, Comput. Struct. 8 (3) (1978) 391–397, http://dx.doi.org/10.1016/0045-7949(78)90183-9.

[60] J. Bonet, R.D. Wood, Nonlinear Continuum Mechanics for Finite Element Analysis, Cambridge University Press, 1997.

[61] B. Vratanar, M. Saje, A consistent equilibrium in a cross-section of an elastic-plastic beam, Int. J. Solids Struct. ASCE 36 (7) (1998) 311–337, http://dx.doi.org/10.1007/BF01602645.

[62] K. Washizu, Variational Methods in Elasticity and Plasticity, Pergamon Press, Paris, 1994.

[63] B. Fortuna, G. Turk, S. Schnabl, Analytical solution of a composite beam with finger joints and incomplete interaction between the layers, Acta Mech. 232 (2021) 4405–4427, http://dx.doi.org/10.1007/s00707-021-03061-x.

[64] CEN, EN 408: 2010+A1: 2012 timber structures - structural timber and glued laminated timber - determination of some physical and mechanical properties, 2010, (In English language).

[65] B. Fortuna, M. Plos, T. Šuligoj, G. Turk, Mechanical properties of slovenian structural beech timber, in: WCTE 2018: Proceedings, World conference on timber engineering.